

UDC 539.3

COMPARATIVE ANALYSIS OF THE USE OF Matlab TOOLS FOR OPTIMIZING PARAMETERS WITH CONSTRAINTS

P.P. Lizunov

O.S. Pogorelova

T.G. Postnikova

Kyiv National University of Construction and Architecture, Kyiv, Ukraine

DOI: 10.32347/2410-2547.2026.116.13-25

A single-sided vibro-impact nonlinear energy sink with high stiffness, which is chosen to eliminate direct damper impacts on the primary structure, requires such optimization of its parameters when the limitations are assigned on both the system parameters and the displacements obtained by integrating the motion equations. In this paper, parameter optimization with constraints is performed using the Matlab platform tools, namely using the *surf* and *fminsearch* programs.

Keywords: vibro-impact, damper, nonlinear energy sink, optimization, constraint, Matlab platform tools.

1. Introduction

Optimization of parameters with constraints is necessitated to optimize the parameters of a single-sided vibro-impact nonlinear energy sink (SSVI NES) of a certain special design.

A nonlinear energy sink is a lightweight device of passive vibration control designed for mitigating the vibration of heavy primary structure (PS). Analytical, experimental, and numerical investigations of many various NES types have been extensively discussed in the global scientific literature over the past two decades [1-3].

The study [4] investigates the use of bistable nonlinear energy sinks (BNES) to suppress multimodal vibrations in axially moving beams. The investigation focused on evaluating how various BNES configurations influence the suppression of multimode vibrations. The effects of key system parameters, including axial velocity, tensile force, external excitation, stiffness, and damping, were systematically analyzed.

Vibro-impact NES (VI NES), that is, vibro-impact damper, is one of NES types.

The study [5] introduces a novel vibration suppression system by combining a TMD with Inerter (TMDI) and a VI NES in a parallel configuration. In this model, the VI NES is a ball inside a cavity within the LO, which hits both cavity walls. The damping coefficient of the VI NES is characterized by the restitution coefficient. The Newtonian impact law and the momentum conservation govern the impulse dynamics. Therefore, when studying parameter changes, the influence of the restitution coefficient is examined, as well as the effect of changing the damping coefficient. The authors believe that the combined use of TMDI and VI NES significantly enhances vibration suppression performance.

In [6], the authors examine the effectiveness of Vibro-Impact Nonlinear Energy Sink cells (VI NES cells) in suppressing multi-mode vibration. The NES units, which are a series of lightweight NES units strategically integrated into the host structures are also defined as NES cells. The effectiveness of VI NES cells is highly sensitive to contact stiffness, mass ratio, and impact gap, necessitating precise tuning of these parameters. Optimizing vibration suppression performance of VI NES cells is performed using Algorithm 1 and Algorithm 2. The vibro-impact process adopts the Hertzian contact theory and use the Hunt and Crossley model to represent the impact interactions as a linear spring with stiffness k and a linear damping with coefficient c . The authors compare the VI-NES with the softened and hard contact. They highlight that the targeted energy transfer performance of VI NES cells can be tuned by selecting appropriate contact stiffness and optimizing the gap parameter.

When coupling a VI NES to a PS, this system becomes strongly nonlinear due to the repeated damper impacts on the obstacles. The strongly system nonlinearity facilitates targeted energy transfer (TET) from the PS to the NES. As a result of this transfer, the PS energy is reduced and its vibrations are mitigated.

When connecting a VI NES to a PS, the structure may contain one or two obstacles, so there are double-sided and single-sided VI NES (DSVI and SSVI NES). SSVI NES is considered an effective device; a lot of works are devoted to its study. In [7, 8], the authors consider a system model that is a linear oscillator (LO) under harmonic excitation with an embedded SSVI NES in the form of a ball inside a cavity within the LO. The ball only hits the right wall of the cavity. To simulate the impact, the authors follow the Hunt and Crossley model, which divides the contact force into two parts: elastic force and damping force. A detailed analysis was performed to uncover the forced behavior of the SSVI NES and provide guidelines for its optimal design in passive vibration suppression as well as the design rules for optimal vibration reduction. “Changing the SSVI-NES parameters is fundamentally about changing the efficiency of energy transfer and dissipation, so the main focus is on two parameters, the linear stiffness and the loss coefficient of the impact process”.

A single-sided vibro-impact bistable NES (SSVI BNES) designed for pulse and seismic control is examined in [9, 10]. The asymmetric SSVI-BNES model is attached to the primary structure on the top floor of a two-story in [9] and an n-story in [10] constructions. From the point of view of our study it is important to note that the obstacle for SSVI BNES is located to the left from it, and its movement to the right is free, and its displacements are not limited. When characterizing the energy dissipation, authors show that “the optimized parameters of the SSVI-BNES are highly sensitive to the changes in initial velocity, while less sensitive to the stiffness of the primary structure”. The authors compare vibration control efficiency of SSVI BNES and TMD and argue that SSVI BNES demonstrates superior vibration reduction performance compared to TMD across most parameter variations.

The study [11] proposes a serial single-sided vibro-impact bistable NES ((SSVI BNES) to solve effectively the issues of energy sensitivity. The parameters of the SSSVI-BNES are optimized using an improved adaptive genetic algorithm (LAGA). The post-collision velocities are determined based on the principles of momentum conservation, displacement continuity, and the velocity recovery. It is worth noting that in this work the damper movement away from the obstacle is also free and unlimited.

Most studies discuss only the damper impacts on the obstacle; the damper movement away the obstacle is not considered. However, the damper behavior as it moves in the direction opposite to the obstacle greatly affects the system dynamics and the reduction of PS energy. In our previous works [12, 13], we studied the dynamics and efficiency in mitigating the PS vibrations using a SSVI NES, when the chosen model, presented in many papers [14 - 17], allowed not only impacts on an obstacle, but also direct damper impacts on the PS and, therefore, demonstrated bilateral impacts, i.e. it operated similar to DSVI NES. However, you can also choose other models that only allow unilateral single-sided impacts on an obstacle. The variants of such models are shown and described in Section 2 in Fig. 1. In this work, we consider only the model shown in Fig. 1 (b). We believe that direct damper impacts on the PS should be eliminated thanks to the design of the SSVI NES model. This is only possible if the stiffness of the connecting spring is sufficiently high. The condition of such direct impact absence imposes restrictions on both the system parameters and the values of variables obtained as a result of integrating the motion equations. The selection of such parameters requires performing the optimization procedure with constraints. In this paper, we demonstrate the use of various Matlab platform tools [18] for such optimization.

2. Description of possible SSVI NES models

To address the challenges related to the damper movement in direction opposite the obstacle, we suggest considering several possible SSVI NES models presented in Fig. 1. They will allow us to analyze various options for damper behavior during its movement in direction opposite the obstacle. The obstacle is rigidly connected to the PS. The exciting force is harmonic $F(t) = P \cos(\omega t + \varphi_0)$, $T = 2\pi / \omega$.

The model in Fig. 1 (a) allows for the damper impacts on both an obstacle rigidly connected to the PS and on the PS directly. The impacts on the PS occur when the displacements of the bodies are equal $x_1 = x_2$, on an obstacle when $x_2 = x_1 + D + C$. The model in Fig. 1 (b) should not allow direct damper impacts on the PS due to the high stiffness of the connecting spring. Collision avoidance with PS imposes a restriction on the relationship between the displacements of bodies

$$x_1 < x_2. \quad (1)$$

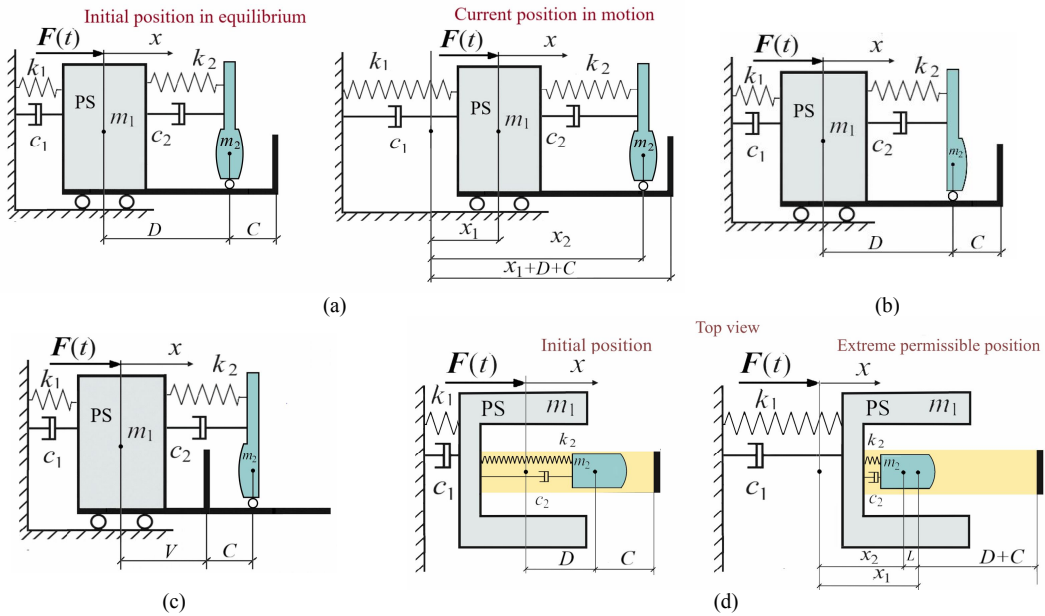


Fig. 1. The schemes of possible models of SSVI NES, which allow occurring of: (a) bilateral impacts; (b) unilateral impacts on an obstacle, direct damper impacts on the PS are prevented due the high stiffness of the connecting spring; (c) unilateral impacts on an obstacle; (d) unilateral impacts on an obstacle, but the restriction on the relationship between the body displacements is more relaxed

In the model shown in Fig. 1 (c), the damper hits an obstacle and its displacements are not restricted. The model in Fig. 1 (d) is similar to the model in Fig. 1 (b), but the restriction on the body displacements is lenient $(x_1 - x_2) \leq L$.

3. Model dynamics when ignoring the direct impacts of the damper on PS

The diagram in Fig. 1 (a) was discussed in our previous works [12,13]. It allows not only impacts on an obstacle but also direct impacts of the SSVI NES on the PS. Let's see how this model behaves if these impacts are ignored. Then the condition of impact occurrence takes the following form

$$x_2 \geq x_1 + (D + C), \text{ that is, } x_2 - x_1 - (D + C) \geq 0 \text{ for impacts on an obstacle.} \quad (2)$$

The motion equations have the following form

$$\begin{aligned} m_1 \ddot{x}_1 + c_1 \dot{x}_1 + k_1 x_1 - c_1 (\dot{x}_2 - \dot{x}_1) - k_2 (x_2 - x_1 - D) &= F(t) + H(z) F_{con}(z), \\ m_2 \ddot{x}_2 + c_2 (\dot{x}_2 - \dot{x}_1) + k_2 (x_2 - x_1 - D) &= -H(z) F_{con}(z). \end{aligned} \quad (3)$$

The initial conditions are:

$$x_1(0) = 0, \quad x_2(0) = D, \quad \dot{x}_1(0) = \dot{x}_2(0) = 0.$$

Here z is the rapprochement of the damper and an obstacle during an impact

$$z = x_2 - x_1 - (D + C). \quad (4)$$

$H(z)$ is the Heaviside function. $F_{con}(z)$ – the contact force that acts only during an impact. According to the Hertz's quasi-static contact theory [19], it has the following form

$$F_{con}(z) = K[z(t)]^{3/2}, \quad (5)$$

where coefficient K characterizes the mechanical and geometrical properties of colliding surfaces:

$$K = \frac{4}{3} \frac{q_1}{(\delta_1 + \delta_2) \sqrt{A + B}}, \quad \delta_1 = \frac{1 - \nu_1^2}{E_1 \pi}, \quad \delta_2 = \frac{1 - \nu_2^2}{E_2 \pi}. \quad (6)$$

Here E_1, E_2 are the Young's moduli of the obstacle surface and the damper colliding surface; ν_1 and ν_2 are their Poisson's coefficients.

The total mechanical energy is calculated using the standard formula.

For PS
$$E_{1total}(t) = E_{1kinetic}(t) + E_{1poten}(t) = \frac{m_1 \dot{x}_1(t)^2 + k_1 x_1(t)^2}{2} \tag{7}$$

For SSVI NES
$$E_{2total}(t) = E_{2kinetic}(t) + E_{2poten}(t) = \frac{m_2 \dot{x}_2(t)^2 + k_2 x_2(t)^2}{2}$$

The structural parameters are taken as follows: $m_1 = 1000$ kg, $k_1 = 3.95 \cdot 10^4$ N/m, $c_1 = 452$ N·s/m, $E_1 = 2.1 \cdot 10^{11}$ N/m², $E_2 = 2.05 \cdot 10^7$ N/m², $\nu_1 = 0.3$, $\nu_2 = 0.4$, $P = 800$ N. The damper mass is $m_2 = 60$ kg that is 6% of PS mass m_1 .

The optimization procedures proposed the damper parameters presented in Table 1.

Table 1

Optimized parameters for SSVI NES in Fig. 1 (a), if we ignore its direct impacts on PS

k_2 , N/m	c_2 , N·s/m	D , m	C , m
600	52	0.06	0.01

The SSVI NES with these parameters provide the behavior of the maximum PS energy as function of exciting force frequency that is shown in Fig. 2 (a). The SSVI NES hits an obstacle over the entire frequency range, which is shown in blue. In Fig. 2 (b), this behavior is compared with that of SSVI NES, which hits both the obstacle and PS directly, i.e. performs bilateral impacts. The dynamics of the system with this damper has been studied in detail in our previous works [12, 13]. The maximum energy of the SSVI NES E_{2max} is also shown in this Fig.

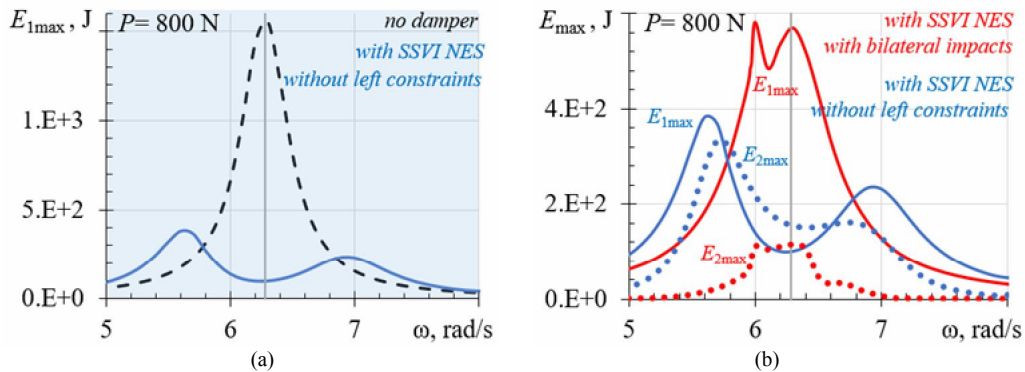


Fig. 2. Reduction of maximum mechanical energy of the PS E_{1max} using SSVI NES: (a) without restrictions on its left displacements; (b) without restrictions in blue and with bilateral impacts on both the obstacle and PS directly in red; the maximum energy of the damper E_{2max} is shown by dotted curves

As can be seen in Fig. 2, the reduction in energy of PS with damper without left constraints is very significant; its maximum energy E_{2max} is huge. Ignoring the direct damper impacts on the PS demonstrates these impressive results. However, it is necessary to find out why the energy of such a small damper has become so large. Fig. 3 demonstrates the displacements of the SSVI NES x_2 as function of time at $P=800$ N and $\omega=6.28$ rad/s.

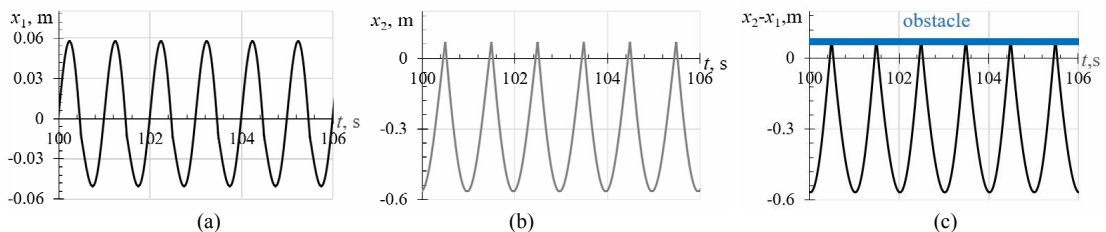


Fig. 3. At $P=800$ N, $\omega=6.28$ rad/s the displacements of: (a) PS; (b) SSVI NES without left constraints; (c) relative displacements, impacts with the obstacle occur at $(x_2 - x_1) = D + C = 0.07$ m

Its displacements x_2 are limited when moving to the right by the presence of an obstacle. According to the diagram in Fig. 1 (a), its leftward displacements should be limited by the presence of PS. However, if we ignore its collision with PS, these displacements become unlimited. Fig. 3 (b) demonstrates the enormous displacements of the damper when moving left in the PS direction, which cannot be realistic due to the presence of PS. It is precisely these enormous unrealistic displacements that provide the damper energy $E_{2\max}$ such huge significance. However, it is precisely this unrestricted free movement of the damper that provides such a significant reduction in maximum PS energy in the resonance zone. It was this circumstance that forced us to analyze other model options for the SSVI NES.

The model shown in Fig. 1 (b) should not allow damper impacts on the PS directly due to the high stiffness of the connected spring k_2 . Collision avoidance imposes the restriction on the relationship between the displacements of the PS x_1 and the damper x_2 as follows: $x_1 < x_2$; they are found by integrating the motion equations (3). Then, when optimizing the damper parameters, this limitation must be taken into account, i.e. we must perform optimization procedures with constraints. We propose using the *Matlab* platform tools for this complex optimization.

We choose the maximum PS energy as the objective function. Limiting the leftward displacements of the damper requires a significant increase in its stiffness k_2 . However, with high stiffness the external load with an amplitude of $P=800$ N proved insufficient for the vibro-impact damper to operate. The motion modes were shock-free. Therefore, we decided to analyze the system behavior at a higher exciting force amplitude, for example, at $P=2000$ N.

4. Determining of approximate parameter values

The relationship between the approximate damper parameters can be found using the *surf* program. The value of the objective function is calculated within this program and displayed on a surface or plane using different colors.

4.1. Calculating of the objective function at exciting force frequency $\omega=6.28$ rad/s and $P=2000$ N

The exciting force frequency $\omega=6.28$ rad/s is the resonant frequency for PS without a damper; therefore, it is advisable to calculate the objective function at this frequency. The figures obtained using the *surf* program and showing the relationships between various damper parameters are presented in Fig. 4 and Fig. 5. Fig. 4 (a) determines three zones of system behavior. The red zone is the area where the damper hits an obstacle. The gray zone is the area in which the damper does not hit an obstacle and the system moves without impacts. The white zone is the area in which the limitation for displacements (1) is not met, this combination of parameters cannot be accepted. Fig. 4 (b) demonstrates the change in maximum PS energy in these zones in color.

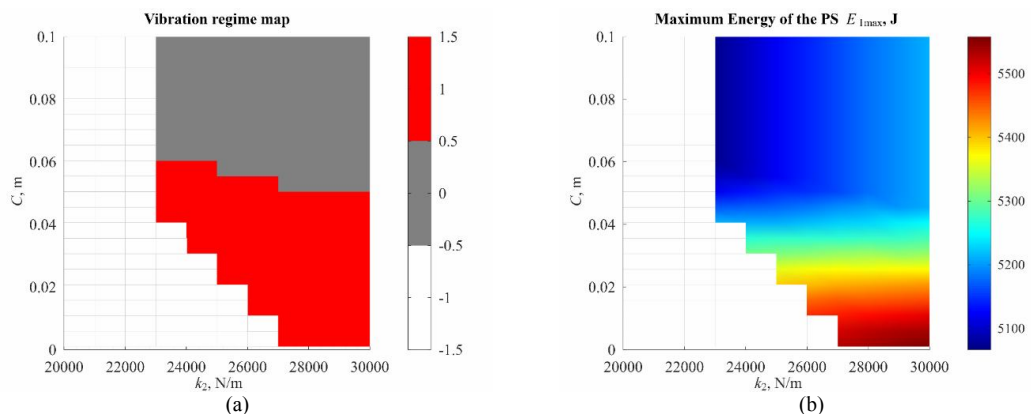


Fig. 4. Identifying areas with different system behavior using the *surf* program based on the relationship between parameters (k_2 – C) at $\omega=6.28$ rad/s and $P=2000$ N

After selecting the clearance value $C=0.03$ m from the graph in Fig. 4 (b), similar images were obtained for the relationship of the parameters ($k_2 - c_2$).

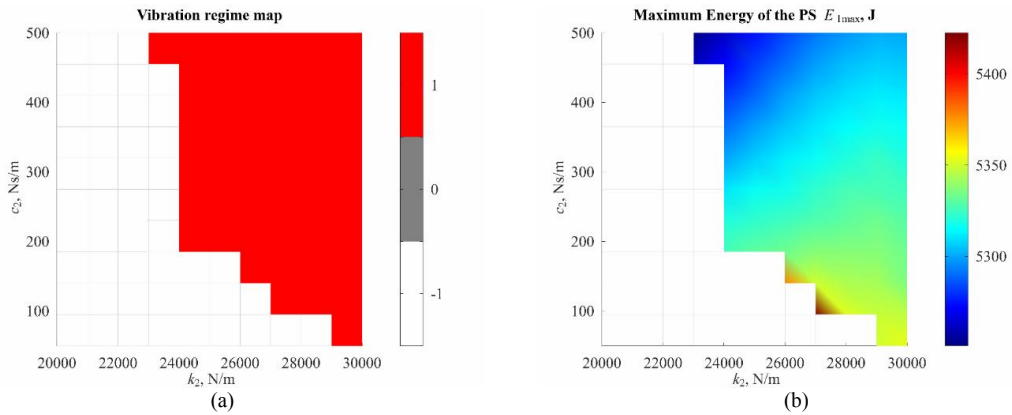


Fig. 5. Identifying areas with different system behavior using the *surf* program based on the relationship between parameters ($k_2^\circ - c_2$) at $\omega=6.28$ rad/s and $P=2000$ N

These approximate parameter values allow you to select their initial values and acceptable limits of change, which will be used for further optimization using one of the *Matlab* platform algorithms. The chosen initial parameter values and limits of changes are shown in Table 2.

Table 2

Optimized parameters for SSVI NES in Fig. 1 (a), if we ignore its direct impacts on PS when calculating the objective function at exciting force frequency $\omega=6.28$ rad/s

Parameter	C, m	$c_2, N \cdot s/m$	$k_2, N/m$
Initial value	0.03	315	27000
Lower limit	0.001	120	26000
Upper limit	0.05	500	29000

4.2. Calculating of the objective function at exciting force frequency $\omega=6.10$ rad/s

Since the resonance of PS with the damper attached shifts to left towards lower frequencies, it is advisable to carry out optimization procedures for exciting force frequency $\omega=6.10$ rad/s.

The figures obtained using the *surf* program, which reflect the approximate relationship between the damper parameters, are presented in Figs. 6 and 7. It should be noted that they differ from those shown in Figs. 4 and 5, despite the small difference in frequency values.

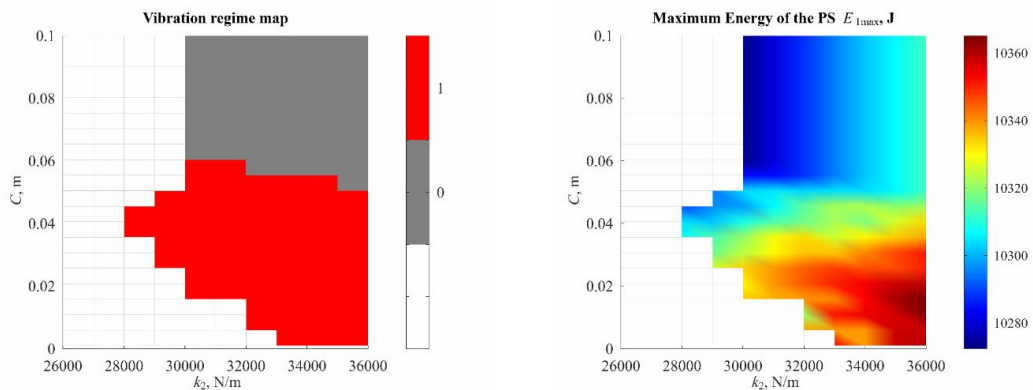


Fig. 6. Identifying areas with different system behavior using the *surf* program based on the relationship between parameters ($k_2^\circ - C$) at $\omega=6.10$ rad/s and $P=2000$ N

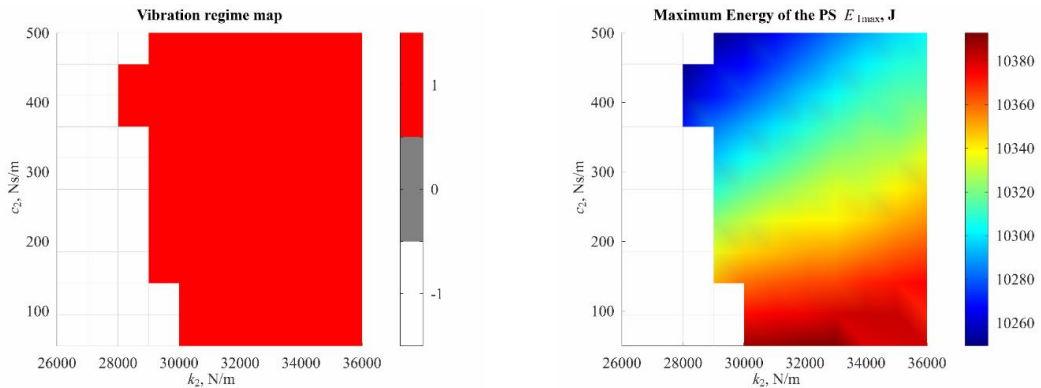


Fig. 7. Identifying areas with different system behavior using the *surf* program based on the relationship between parameters $(k_2^2 - c_2)$ at $\omega=6.10$ rad/s and $P=2000$ N

In this case, the chosen initial parameter values and limits of changes are shown in Table 3.

Table 3

Optimized parameters for SSVI NES in Fig. 1 (a), if we ignore its direct impacts on PS when calculating the objective function at exciting force frequency $\omega=6.10$ rad/s

Parameter	C, m	$c_2, N\cdot s/m$	$k_2, N/m$
Initial value	0.03	315	32000
Lower limit	0.001	120	30000
Upper limit	0.05	500	36000

5. Refinement of approximate parameter values

Further optimization and refinement of the found approximate parameter values can be performed using one of the *Matlab* platform algorithms based on their initial values, as well as the lower and upper limits found using the *surf* program.

5.1. Refinement of approximate parameter values using the *fminsearch* program

The *fminsearch* program, based on the Nelder–Mead simplex algorithm, finds a local minimum of the objective function while simultaneously optimizing multiple parameters. Since *fminsearch* is an unconstrained optimization method, constraints on the damper parameters and the displacements of the system bodies, as specified in condition (1), are enforced using penalty terms. The *fminsearch* program assigns *penalty_1* as a large value and adds it to the objective function when at least one parameter exceeds its prescribed range, and *penalty_2* when condition (1) is violated. In this way, infeasible solutions are penalized and the algorithm continues the search using other parameter values.

In the case where the objective function is evaluated at the excitation frequency $\omega=6.28$ rad/s and with an external load intensity of $P=2000$ N, a fragment of the program operation is shown below. The standard iterative output was disabled, and a custom printout mechanism was employed to monitor the optimization process by reporting the current values of the parameters C, c_2 and k_2 , as well as the physical component of the objective function and the corresponding penalty terms. Fragment of the program operation looks like this:

Fragment of *fminsearch* Algorithm Operation (Sets 1–2)

Iter	C, m	$c_2, Ns/m$	$k_2, N/m$	E_{1phys}, J	<i>penalty_1</i>	<i>penalty_2</i>	Objective E_{1max}, J	
1	0.03000	315.00	27000.0	5291.704	0.000e+000	0.000e+000	5291.704	Set 1
2	0.03150	315.00	27000.0	5278.386	0.000e+000	0.000e+000	5278.386	
3	0.03000	330.75	27000.0	5290.595	0.000e+000	0.000e+000	5290.595	
4	0.03100	325.50	25650.0	5275.885	1.225e+013	0.000e+000	12250000005275.885	
5	0.03025	317.63	27675.0	5291.442	0.000e+000	0.000e+000	5291.442	
....	
435	0.04996	499.39	25998.3	5093.805	3.054e+008	0.000e+000	305436289.682	
436	0.04996	499.54	25998.2	5093.791	3.385e+008	0.000e+000	338526605.435	

437	0.04995	499.74	26004.0	5093.894	0.000e+000	0.000e+000	5093.894	
438	0.04995	499.60	26000.1	5093.825	0.000e+000	0.000e+000	5093.825	Set 2

Optimal solution (*fminsearch*): $C = 0.04995$ m, $c_2 = 499.60$ Ns/m, $k_2 = 26000.1$ N/m, $E_{1max} = 5093.825$ J

As result of optimization, two sets of parameters were selected.

Table 4

The sets of optimized parameters for SSVI NES with large stiffness found at $\omega=6.28$ rad/s and $P=2000^\circ\text{N}$

Parameter	C , m	c_2 , N·s/m	k_2 , N/m	E_{1max} , J
Set 1	0.03000	315.00	27000.0	5291.704
Set 2	0.04995	499.60	26000.1	5093.825

The SSVI NESs with these parameters provide the behavior of maximum PS energy shown in Fig. 8. The resonance shifts to left towards lower frequencies and does not decrease, but even increases slightly. The maximum PS energy decreases for higher frequencies; at the same time, the energy increases for lower frequencies. Despite the fact that the optimization procedures performed for exciting force frequency $\omega=6.28$ rad/s rejected parameter values that did not satisfy the condition (1), such a violation occurred for another frequency $\omega=6.1$ rad/s corresponding a new resonance. In Figs. 8 (a), (b), the region in which condition (1) is not satisfied is shown in pink. In blue zones, SSVI NES hits an obstacle; in white areas, the motion occurs without impacts. Fig. 8 (c) shows the complete coincidence of the energy curves for SSVI NESs with two different sets of parameters.

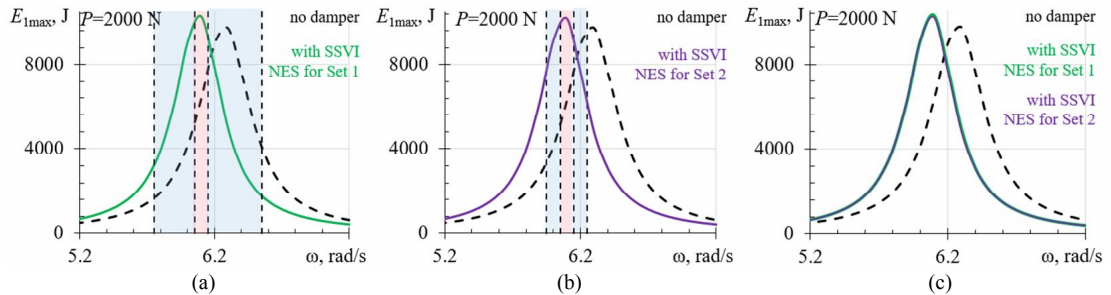


Fig. 8. The behavior of the maximum energy of PS coupled with SSVI NESs with two different sets of parameters for: (a) Set 1, (b) Set 2, (c) comparison of energy curves for Set 1 and Set 2

Since the resonance shifts to left towards lower frequencies, it is indeed advisable to carry out optimization procedures for exciting force frequency $\omega=6.10$ rad/s and use the results presented in Table 3 in Subsection 4.2. The further parameter optimization using the *fminsearch* program with penalty assignment determines two new sets of damper parameters:

Fragment of *fminsearch* Algorithm Operation (Sets 3–4)

Iter	C , m	c_2 , Ns/m	k_2 , N/m	E_{1phys} , J	penalty 1	penalty 2	Objective E_{1max} , J	
1	0.03000	315.00	32000.0	10316.167	0.000e+000	0.000e+000	10316.167	Set 3
2	0.03150	315.00	32000.0	10314.946	0.000e+000	0.000e+000	10314.946	
3	0.03000	330.75	32000.0	10312.305	0.000e+000	0.000e+000	10312.305	
4	0.03100	325.5	30400.0	10303.026	0.000e+000	0.000e+000	10303.026	
5	0.03150	330.75	28800.0	10288.254	1.440e+014	0.000e+000	144000000010288.250	
....	
44	0.03032	509.03	30748.7	10256.927	8.159e+009	0.000e+000	8158549289.722	
45	0.03097	463.51	30599.8	10268.261	0.000e+000	0.000e+000	10268.261	
46	0.03054	493.86	30699.0	10260.576	0.000e+000	0.000e+000	10260.576	Set 4

Optimal solution (*fminsearch*): $C = 0.03054$ m, $c_2 = 493.86$ Ns/m, $k_2 = 30699.0$ N/m, $E_{1max} = 10260.576$ J

The parameter values for Set 3 and Set 4 are summarized in Table 5.

Table 5

The sets of optimized parameters for SSVI NES with large stiffness found at $\omega=6.10$ rad/s and $P=2000^\circ\text{N}$

Parameter	$C, \text{ m}$	$c_2, \text{ N}\cdot\text{s/m}$	$k_2, \text{ N/m}$	$E_{1\text{max}}, \text{ J}$
Set 3	0.03000	315.00	32000.0	10316.167
Set 4	0.03054	493.86	30699.0	10260.576

The SSVI NESs with these parameters provide the behavior of maximum PS energy shown in Fig. 9. These graphs differ from those in Fig. 8 in only one aspect, namely, they do not have pink areas, i.e. the condition (1) is satisfied across the entire frequency range. As in Fig. 8, the resonance here also shifts to left towards lower frequencies and does not decrease, but even increases slightly. The maximum PS energy decreases for higher frequencies; at the same time, the energy increases for lower frequencies. These phenomena persist despite the fact that the parameters were optimized at another frequency and received other values.

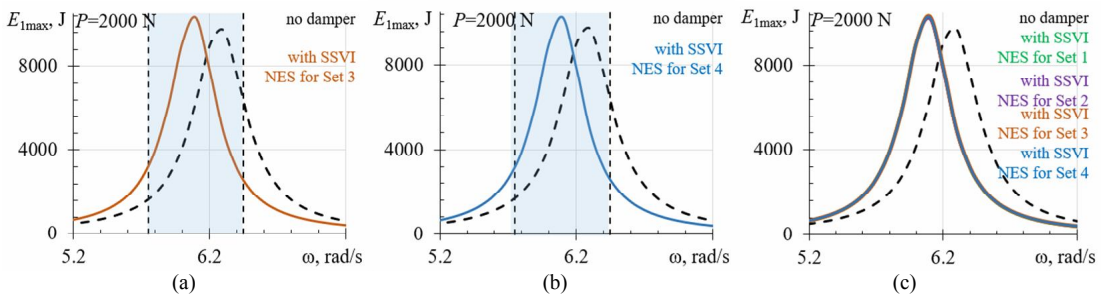


Fig. 9. The behavior of the maximum energy of PS coupled with SSVI NESs with two different sets of parameters for: (a) Set 3, (b) Set 4, (c) comparison of energy curves for Set 1, Set 2, Set 3, and Set 4

It is worth noting that the energy curves coincide completely for all four sets of parameters as shown in Fig. 9 (c).

Thus, the SSVI NES model with high stiffness, which prevents direct damper impacts on PS, is not a good option, as it shows worse results than the model with bilateral impacts, as demonstrated in Fig. 2 (b).

5.2. Refinement of approximate parameter values using the *fmincon* program

The *fmincon* program employs other algorithms to find a local minimum of the objective function. However, from the user’s perspective, this program is similar to *fminsearch*. The user specifies the initial values of the parameters to be optimized, as well as their acceptable bounds. The program enforces condition (1) for the constraints on the displacements of the system bodies and assigns a penalty if this condition is violated. Parameter bounds are enforced internally by the program, and no penalty is assigned for exceeding them.

During the optimization process, the standard iterative output of *fmincon* was enabled, providing information on the objective function value and constraint satisfaction at each iteration. In addition to the standard solver output, a custom logging routine was implemented to print selected intermediate optimization variables and objective-related quantities at each iteration. This output included the current values of the design parameters (C, c_2, k_2) the maximum energy measure $E_{1\text{max}}$ and the *penalty* term. When the objective function is calculated at $P=2000$ N and $\omega=6.28$ rad/s, the fragment of the *fmincon* program operation looks like this:

Selected intermediate iterations of the *fmincon* optimization procedure

Iter	$C, \text{ m}$	$c_2, \text{ N}\cdot\text{s/m}$	$k_2, \text{ N/m}$	$E_{1\text{max}}, \text{ J}$	<i>penalty</i>
1	0.030000	315.000000	27000.000000	5410.709000	0.000000
2	0.050000	286.028000	27000.087000	5297.753000	0.000000
...
84	0.049999	286.028000	27000.087000	5297.753000	0.000000

Iter	C, m	$c_2, Ns/m$	$k_2, N/m$	E_{1max}, J	penalty
85	0.050000	286.028000	27000.087000	5297.753000	0.000000
86	0.050000	286.028000	27000.087000	5297.753000	0.000000

Final optimal solution of the constrained optimization problem

Iter	F-count	$f(x)$	Feasibility	Steplength	Step	Norm of First-order optimality
0	4	5410.710000	0.000000			12050.000000
1	8	5297.753000	0.000000	1.000000	28.980000	5652.000000
2	47	5297.753000	0.000000	0.000004	0.000629	16970.000000
3	87	5297.753000	0.000000	0.000001	0.000010	16970.000000

Optimal solution (*fmincon*): $C = 0.050000$ m, $c_2 = 286.027783$ Ns/m, $k_2 = 27000.865621$ N/m, $E_{1max} = 5297.752609$ J

Running the program in two variants with two different sets of initial parameter values provided set of optimized parameters with a minimum objective function value $E_{1max} = 5298$ J. Under the same conditions the *fminsearch* program found optimized parameter set with a minimum objective function value $E_{1max} = 5094$ J. For this reason alone, we preferred to use the *fminsearch* program in our strongly nonlinear problem involving impacts and contact mechanics.

5.3. Refinement of approximate parameter values using the *Ga* algorithm

Approximate parameter values can also be refined using the GA (Genetic Algorithm). For this algorithm, the initial parameter values are not specified, but restrictions on the parameter values are enforced. Condition (1) is checked, and if it is violated, a penalty is assigned. There are many sets of parameters that provide similar performance and efficiency for a vibro-impact damper coupled to the primary structure. The GA uses random numbers during its operation, so it produces different parameter sets at each run, which nevertheless correspond to local minima of the objective function.

The standard GA output provides information on the best objective function value at each generation and convergence status. In addition, a custom logging routine can be implemented to track intermediate values of selected optimization parameters and objective-related quantities at each generation. This allows monitoring the evolution of the parameter sets and the corresponding objective function and penalty values throughout the optimization process.

When the objective function is calculated at $P=2000$ N and $\omega=6.28$ rad/s, the fragment of *Ga* algorithm operation looks like this:

Monitoring of optimization parameters, objective function, and penalty values at selected generations

C, m	$c_2, Ns/m$	$k_2, N/m$	E_{1max}, J	penalty	Objective E_{1max}, J
5.000000E-02	1.200000E+02	2.600000E+04	5.314390E+03	0.000000E+00	5.314390E+03
3.639283E-03	4.904377E+02	2.897708E+04	5.582097E+03	0.000000E+00	5.582097E+03
2.311737E-02	3.430673E+02	2.727268E+04	5.458593E+03	0.000000E+00	5.458593E+03
1.974967E-02	2.772769E+02	2.818659E+04	5.497516E+03	0.000000E+00	5.497516E+03
1.885006E-02	2.202569E+02	2.842697E+04	5.518067E+03	0.000000E+00	5.518067E+03
2.708515E-02	4.083312E+02	2.706953E+04	5.412501E+03	0.000000E+00	5.412501E+03
4.370235E-02	1.908971E+02	2.777297E+04	5.351538E+03	0.000000E+00	5.351538E+03
3.285578E-02	1.944032E+02	2.658130E+04	5.393129E+03	0.000000E+00	5.393129E+03

ga optimization progress over generations

Generation	f-count	Best $f(x)$	Mean $f(x)$	Stall Generations
1	24	5269	5370	0
2	36	5269	5328	1
3	48	5269	5317	2
4	60	5269	5304	3
5	72	5269	5296	4
6	84	5269	5318	0
7	96	5269	5300	1

Optimal solution (*ga*): $C = 0.050000$ m, $c_2 = 498.432073$ Ns/m, $k_2 = 26000.000000$ N/m, $E_{1max} = 5269.185561$ J

During operation, *Ga* offers various parameter sets; the dynamics of each of them should be analysed to select the most successful one. The minimum value of the objective function found using *Ga* is $E_{1\max} = 5269$ J, what is less than the value found by the *fmincon* program, but greater than that found by the *fminsearch* program. These circumstances also influenced our decision to use the *fminsearch* program to further refine the approximate parameter values.

6. Conclusions

This study suggests focusing on dynamic behavior, specifically the displacements of the SSVI NES as it moves in direction opposite the obstacle. We have shown that the damper leftward displacements are too large if its direct impacts on the PS are ignored. We examined this model when a very high damper stiffness was selected to eliminate these impacts. However, to determine the optimized parameters for this model, it was necessary to perform optimization procedures with constraints on both the system parameters and displacements, which are variables obtaining by integrating the motion equations. In this paper, optimization procedures were performed using *Matlab* platform tools. The approximate damper parameters were determined using the *surf* program, which constructs an image where the dependence of the objective function value on the relationship between two parameters is displayed in color. The selected approximate parameters should be further optimized; their values can be refined using various *Matlab* platform tools. We compared the use of *fminsearch* and *fmincon* programs, as well as the *Ga* genetic algorithm, and chose the *fminsearch* program. Using the *fminsearch* program with a penalty for violating the constraint conditions gives quite good results and allows us to select several sets of optimized damper parameters. However, the analysis of the efficiency in mitigating the PS vibrations for SSVI NESs with four sets of optimized parameters showed that such a model with high stiffness of connecting spring could hardly be considered successful.

REFERENCES

1. Fang Y., Ma X., Xia X., Yu R., Zhong Y., Zhang Z. Dynamics-guided constrained optimization of a piezoelectric nonlinear energy sink for structural vibration control // *Engineering Structures*. – 2026. – Vol. 346. – Art. no. 121668. – DOI: <https://doi.org/10.1016/j.engstruct.2025.121668>.
2. Li X., Qin Y., Lin X., Wang Z., Wang L., Yan Z., Nie X. Parameter optimization and vibration control of tristable nonlinear energy sink incorporating with linear and nonlinear damping under impact excitation // *International Journal of Dynamics and Control*. – 2025. – Vol. 13, No. 12. – DOI: <https://doi.org/10.1007/s40435-025-01942-w>.
3. Abdollahi, A.; Bab, S. Improving vibration suppression by applying stochastic optimization to a coil-contained vibro-impact nonlinear energy sink within a linear oscillator framework. *Appl. Math. Model.* 2026, 151, 116479. <https://doi.org/10.1016/j.apm.2025.116479>
4. Chen P., Yang J.-H., Guo X.-Y., Liu H.-T., Yang X.-D. Vibration analysis and vibration reduction strategy for an axially moving beam with a bistable nonlinear energy sink // *European Journal of Mechanics – A/Solids*. – 2026. – Vol. 117. – Art. no. 106029. – DOI: <https://doi.org/10.1016/j.euromechsol.2026.106029>
5. Abdollahi A., Malekzadeh M. Enhancing vibration control: A parallel integration of tuned mass damper with inerter and vibro-impact nonlinear energy sink // *Chaos, Solitons & Fractals*. – 2026. – Vol. 203. – Art. no. 117658. – DOI: <https://doi.org/10.1016/j.chaos.2025.117658>
6. Jiang X., Lu Z.-R., Lin X., Yuan J., Wang L., Yang D. An event-driven time-domain sensitivity method for optimizing parameters of vibro-impact NES cells to suppress multi-mode vibration // *Journal of Sound and Vibration*. – 2026. – Vol. 628. – Art. no. 119664. – DOI: <https://doi.org/10.1016/j.jsv.2026.119664>
7. Lin Z., Li H., Li A., Zhang Z., Kong X., Ding Q. Dynamic analysis of single-sided vibro-impact nonlinear energy sinks via forced response curves and application to vibration mitigation // *Journal of Sound and Vibration*. – 2025. – Vol. 612. – Art. no. 119150. – DOI: <https://doi.org/10.1016/j.jsv.2025.119150>
8. Lin Z., Li H., Li S., He M., Ma Z., Ding Q. An analytical investigation on the vibration suppression performance of the single-sided vibro-impact nonlinear energy sink // *Journal of Vibration Engineering & Technologies*. – 2024. – Vol. 12, No. 7. – P. 8067–8082. – DOI: <https://doi.org/10.1007/s42417-024-01345-9>
9. Li J., Li S.-B., Yu G.-L., Zhu L. A single-sided vibro-impact bistable nonlinear energy sink designed for pulse and seismic control // *Structures*. – 2025. – Vol. 71. – Art. no. 107958. – DOI: <https://doi.org/10.1016/j.istruc.2024.107958>
10. Li J., Sun B.-X., Yu G.-L. Vibration mitigation for high-rise buildings by a single-sided vibro-impact bistable nonlinear energy sink // *Soil Dynamics and Earthquake Engineering*. – 2026. – Vol. 203. – Art. no. 110083. – DOI: <https://doi.org/10.1016/j.soildyn.2025.110083>
11. Li J., Yu G.-L. Enhanced vibration suppression of structures using an optimized serial single-sided vibro-impact bistable NES // *Communications in Nonlinear Science and Numerical Simulation*. – 2026. – Art. no. 109763. – DOI: <https://doi.org/10.1016/j.cnsns.2026.109763>
12. Lizunov P., Pogorelova O., Postnikova T. Tuning of vibro-impact nonlinear energy sinks under changing structural parameters. Part 2. Comparison with tuned mass dampers // *Strength of Materials and Theory of Structures*. – 2025. – No. 115. – P. 13–32. – DOI: <https://doi.org/10.32347/2410-2547.2025.115.13-32>

13. Lizunov P., Pogorelova O., Postnikova T. Retention of tuning for vibro-impact and linear dampers under periodic excitation // Preprints. – 2025. – DOI: <https://doi.org/10.20944/preprints202512.2637.v1>
14. Wierschem N. E., Hubbard S. A., Luo J., Fahnestock L. A., Spencer B. F., McFarland D. M., Quinn D. D., Vakakis A. F., Bergman L. A. Response attenuation in a large-scale structure subjected to blast excitation utilizing a system of essentially nonlinear vibration absorbers // Journal of Sound and Vibration. – 2017. – Vol. 389. – P. 52–72. – DOI: <https://doi.org/10.1016/j.jsv.2016.11.003>
15. Li T., Seguy S., Berlioz A. On the dynamics around targeted energy transfer for vibro-impact nonlinear energy sink // Nonlinear Dynamics. – 2016. – Vol. 87, No. 3. – P. 1453–1466. – DOI: <https://doi.org/10.1007/s11071-016-3127-0>
16. Al-Shudeifat M. A., Wierschem N., Quinn D. D., Vakakis A. F., Bergman L. A., Spencer B. F. Numerical and experimental investigation of a highly effective single-sided vibro-impact nonlinear energy sink for shock mitigation // International Journal of Non-Linear Mechanics. – 2013. – Vol. 52. – P. 96–109. – DOI: <https://doi.org/10.1016/j.ijnonlinmec.2013.02.004>
17. Li W., Wierschem N. E., Li X., Yang T. On the energy transfer mechanism of the single-sided vibro-impact nonlinear energy sink // Journal of Sound and Vibration. – 2018. – Vol. 437. – P. 166–179. – DOI: <https://doi.org/10.1016/j.jsv.2018.08.057>
18. *MathWorks*, MATLAB Documentation. [Online]. Available: <https://www.mathworks.com/help/matlab/>. Accessed: Jan. 27, 2026.
19. Goldsmith W. Impact: the Theory and Physical Behavior of Colliding Solids, Edward Arnold Ltd //London, England. – 1960.

Стаття надійшла 29.01.2026

Лізунов П.П., Погорелова О.С., Постнікова Т.Г.

ПОРІВНЯЛЬНИЙ АНАЛІЗ ВИКОРИСТАННЯ ІНСТРУМЕНТІВ *Matlab* ДЛЯ ОПТИМІЗАЦІЇ ПАРАМЕТРІВ З ОБМЕЖЕННЯМИ.

У цьому дослідженні пропонується зосередитися на динамічній поведінці однобічного віброударного нелінійного поглинач енергії (SSVI NES), коли він рухається у напрямку, протилежному до перешкоди. Він може вдаритися об основну конструкцію (PS); його динаміка та ефективність у зменшенні вібрацій PS були досліджені в наших попередніх роботах. Якщо ці удари просто ігнорувати, демпфер рухається в напрямку PS на дуже велику відстань, що є нереалістичним для цієї діаграми. Щоб запобігти таким ударам, з'єднувальна пружина повинна мати велику жорсткість. Однак при оптимізації параметрів демпфера вимога уникнути цих впливів змушує встановлювати обмеження не тільки на параметри, але й на взаємозв'язок між переміщеннями тіл, які є змінними, отриманими шляхом інтегрування рівнянь руху. Процедури оптимізації виконувалися за допомогою інструментів платформи *Matlab*. Орієнтовні значення параметрів демпфера визначаються за допомогою програми *surf*, яка буде зображення, на якому кольором відображається залежність значення цільової функції від взаємозв'язку між двома параметрами. Вибрані орієнтовні значення параметрів слід додатково оптимізувати; їхні значення можна уточнити за допомогою різних інструментів платформи *Matlab*. Ми порівняли використання програм *fminsearch* та *fmincon*, а також генетичного алгоритму *Ga* й вибрали програму *fminsearch*. Використання програми *fminsearch* з використанням штрафу за порушення умов обмеження дає досить хороші результати та дозволяє вибрати кілька наборів оптимізованих параметрів демпфера. Однак аналіз ефективності зменшень коливань PS для SSVI NES з чотирма різними наборами оптимізованих параметрів показав, що таку модель з великою жорсткістю з'єднувальної пружини вдалою.

Ключові слова: віброудар, демпфер, нелінійний поглинач енергії, оптимізація, обмеження, інструменти платформи *Matlab*.

Lizunov P.P., Pogorelova O.S., Postnikova T.G.

COMPARATIVE ANALYSIS OF THE USE OF *Matlab* TOOLS FOR OPTIMIZING PARAMETERS WITH CONSTRAINTS

This study suggests focusing on dynamic behavior of the single-sided vibro-impact nonlinear energy sink (SSVI NES) as it moves in direction opposite the obstacle. It can hits the primary structure (PS); its dynamics and efficiency in mitigating the PS vibrations were examined in our previous works. If these impacts are simply ignored, the damper moves in the PS direction over a very large distance, which is unrealistic for this diagram. To prevent such impacts, the connecting spring must have high stiffness. However, when optimizing damper parameters, the requirement to avoid these impacts makes it necessary to set limits not only on the parameters, but also on the relationship between the displacements of bodies, which are variables obtained by integrating the motion equations. The optimization procedures were performed using *Matlab* platform tools. The approximate damper parameters are determined using the *surf* program, which constructs an image where the dependence of the objective function value on the relationship between two parameters is displayed in color. The selected approximate parameters should be further optimized; their values can be refined using various *Matlab* platform tools. We compared the use of *fminsearch* and *fmincon* programs, as well as the *Ga* genetic algorithm, and chose the *fminsearch* program. Using the *fminsearch* program with a penalty for violating the constraint conditions gives quite good results and allows us to select several sets of optimized damper parameters. However, the analysis of the efficiency in mitigating the PS vibrations for SSVI NESs with four various sets of optimized parameters showed that such a model with high stiffness of connecting spring could hardly be considered successful.

Keywords: vibro-impact, damper, nonlinear energy sink, optimization, constraint, *Matlab* platform tools.

УДК 539.3

Лізунов П.П., Погорелова О.С., Постнікова Т.Г. Порівняльний аналіз використання інструментів *Matlab* для оптимізації параметрів з обмеженнями // Опір матеріалів і теорія споруд: наук.-тех. збірн. – К.: КНУБА. 2026. – Вип. 116. – С. 13-25. – Англ.

*Однобічний віброударний нелінійний поглинач енергії з великою жорсткістю, який обрано для усунення прямих ударів демпфера на основну конструкцію, вимагає такої оптимізації своїх параметрів, коли обмеження накладаються як на параметри системи, так і на переміщення, отримані шляхом інтегрування рівнянь руху. У цій статті оптимізація параметрів з обмеженнями виконується за допомогою інструментів платформи *Matlab*, а саме за допомогою програм *surf* та *fminsearch*.*

Табл. 5. Іл. 9. Бібліог. 19 назв.

UDC 539.3

Lizunov P.P., Pogorelova O.S., Postnikova T.G. Comparative analysis of the use of *Matlab* tools for optimizing parameters with constraints // Strength of Materials and Theory of Structures: Scientific-and-technical collected articles. – K.: KNUBA. 2026. – Issue 116. – P. 13-25.

A single-sided vibro-impact nonlinear energy sink with high stiffness, which is chosen to eliminate direct damper impacts on the primary structure, requires such optimization of its parameters when the limitations are assigned on both the system parameters and the displacements obtained by integrating the motion equations. In this paper, parameter optimization with constraints is performed using the Matlab platform tools, namely using the surf and fminsearch programs.

Tabl. 5. Figs. 9. Refs. 31.

Автор (науковий ступінь, вчене звання, посада): доктор технічних наук, професор, завідувач кафедри будівельної механіки КНУБА, директор НДІ будівельної механіки ЛІЗУНОВ Петро Петрович

Адреса робоча: 03680 Україна, м. Київ, проспект Повітряних Сил 31, Київський національний університет будівництва і архітектури

Робочий тел.: +38(044) 245-48-29

E-mail: lizunov@knuba.edu.ua

ORCID ID: <http://orcid.org/0000-0003-2924-3025>

Автор (науковий ступінь, вчене звання, посада): кандидат фізико-математичних наук, старший науковий співробітник, провідний науковий співробітник НДІ будівельної механіки КНУБА ПОГОРЕЛОВА Ольга Семенівна

Адреса робоча: 03680 Україна, м. Київ, проспект Повітряних Сил 31, Київський національний університет будівництва і архітектури

Робочий тел.: +38(044) 245-48-29

E-mail: pogos13@ukr.net

ORCID ID: <http://orcid.org/0000-0002-5522-3995>

Автор (науковий ступінь, вчене звання, посада): кандидат технічних наук, старший науковий співробітник, провідний науковий співробітник НДІ будівельної механіки КНУБА ПОСТНІКОВА Тетяна Георгіївна

Адреса робоча: 03680 Україна, м. Київ, проспект Повітряних Сил 31, Київський національний університет будівництва і архітектури

Робочий тел.: +38(044) 245-48-29

E-mail: postnikova.tg@knuba.edu.ua

ORCID ID: <https://orcid.org/0000-0002-6677-4127>